ORIGINAL ARTICLE

# Mutations in *RSPH1* Cause Primary Ciliary Dyskinesia with a Unique Clinical and Ciliary Phenotype

Michael R. Knowles[1], Lawrence E. Ostrowski[1], Margaret W. Leigh[2], Patrick R. Sears[1], Stephanie D. Davis[2]*, Whitney E. Wolf[1], Milan J. Hazucha[1], Johnny L. Carson[2], Kenneth N. Olivier[3], Scott D. Sagel[4], Margaret Rosenfeld[5], Thomas W. Ferkol[6], Sharon D. Dell[7], Carlos E. Milla[8], Scott H. Randell[9], Weining Yin[1], Aruna Sannuti[1], Hilda M. Metjian[1,10], Peadar G. Noone[1], Peter J. Noone[1], Christina A. Olson[1], Michael V. Patrone[1], Hong Dang[1], Hye-Seung Lee[11], Toby W. Hurd[12†], Heon Yung Gee[12‡], Edgar A. Otto[12], Jan Halbritter[12‡], Stefan Kohl[12‡], Martin Kircher[13], Jeffrey Krischer[11], Michael J. Bamshad[13,14], Deborah A. Nickerson[13], Friedhelm Hildebrandt[12,15‡], Jay Shendure[13], and Maimoona A. Zariwala[16]

[1]Department of Medicine, [2]Department of Pediatrics, [9]Department of Cell Biology and Physiology, and [16]Department of Pathology and Laboratory Medicine, University of North Carolina School of Medicine, Chapel Hill, North Carolina; [3]Laboratory of Clinical Infectious Diseases, National Institute of Allergy and Infectious Diseases, Bethesda, Maryland; [4]Department of Pediatrics, University of Colorado School of Medicine, Aurora, Colorado; [5]Seattle Children's Hospital and Department of Pediatrics, [13]Department of Genome Sciences, and [14]Department of Pediatrics, University of Washington School of Medicine, Seattle, Washington; [6]Department of Pediatrics, Washington University School of Medicine, St. Louis, Missouri; [7]Department of Pediatrics, The Hospital for Sick Children, University of Toronto, Toronto, Ontario, Canada; [8]Department of Pediatrics, Stanford University, Palo Alto, California; [10]Raleigh Pulmonary and Allergy, Raleigh, North Carolina; [11]Department of Pediatrics, University of South Florida, Tampa, Florida; [12]Department of Pediatrics, University of Michigan, Ann Arbor, Michigan; and [15]Howard Hughes Medical Institute, Chevy Chase, Maryland

(Received in original form November 20, 2013; accepted in final form January 29, 2014)

*Current address: Section of Pediatric Pulmonology, Allergy and Sleep Medicine, James Whitcomb Riley Hospital for Children, Indiana University School of Medicine, Indianapolis, Indiana.

†Current address: MRC Human Genetics Unit, Institute of Genetics and Molecular Medicine, University of Edinburgh, Edinburgh, United Kingdom.

‡Current address: Division of Nephrology, Department of Medicine, Boston Children's Hospital, Harvard Medical School, Boston, Massachusetts.

Supported by NIH-ORDR-NHLBI grant 5 U54HL096458-06 (M.R.K., M.W.L., J.L.C., M.J.H., S. D. Davis, S. D. Dell, T.W.F., S.D.S., K.N.O., M.R., C.E.M., and M.A.Z), by NIH-NHLBI grants 5R01HL071798 and 1R01HL117836 (M.R.K., L.E.O., and M.A.Z.), by NIH-NHGRI grant 1 U54HG006493 (M.J.B., D.A.N., and J.S.), and by NIH-R01 DK068306 (F.H.). K.N.O. is supported by the Intramural Research Program of the NIH-NIAID. Resequencing was provided through RS&G by NIH-NHLBI contract # HHSN268201100037C. The work was supported by NIH-NCATS grants UL1TR000083 to University of North Carolina, Chapel Hill, UL1TR000154 to University of Colorado CTSI, Cystic Fibrosis Foundation grants CFF R026-CR07 and R026-CR11, and NIH-NIDDK grant P30-DK065988. The content is solely the responsibility of the authors and does not necessarily represent the official view of the NIH.

Author Contributions: All authors have reviewed the manuscript. M.R.K. contributed to the overall study design and execution, patient and clinical information collection, genetics, ciliary ultrastructural and waveform analysis, high-speed microscopy review, and manuscript preparation. M.A.Z. contributed to overall study design and execution, family history evaluation, genetic studies, Sanger sequencing and RNA work, data analysis from multiple sources, and manuscript preparation. L.E.O. contributed to RNA and protein work, high-speed microscopy, epithelial cell cultures, and manuscript preparation. M.W.L. contributed to patient and clinical information collection, ciliary ultrastructural and nasal nitric oxide analysis, and critical review of manuscript. J.S. contributed to whole exome sequencing and analysis and Sanger sequencing and critical review of manuscript. P.R.S. contributed to high-speed video microscopy. S. D. Davis, S. D. Dell, K.N.O., S.D.S., M.R., T.W.F., C.E.M., A.S., H.M.M., and P.G.N. contributed to patient and clinical information collection. W.E.W. contributed to validation studies by Sanger sequencing. M.J.H. contributed to nasal nitric oxide analysis. J.L.C. contributed to ciliary ultrastructural and waveform analysis. S.H.R. helped with human epithelial cell cultures. W.Y. contributed to RNA and protein experiments. P.J.N. and C.A.O. contributed to quantitative analysis of ciliary ultrastructure. M.V.P. assisted with lung function test analysis. H.D. helped with whole exome sequencing data formatting for the analysis. H.-S.L. contributed to lung function calculation and statistical analysis and manuscript review. T.W.H., H.Y.G., E.A.O., J.H., S.K., and F.H. contributed to the RSPH1 screening by whole exome sequencing and/or Fluidigm. M.K., M.J.B., and D.A.N. contributed to whole exome sequencing and analysis and Sanger sequencing. J.K. contributed to Genetic Disorders of Mucociliary Clearance Consortium database oversight and statistical analysis.

Correspondence and requests for reprints should be addressed to Michael R. Knowles, M.D., Cystic Fibrosis Center, 7019 Thurston-Bowles Building, CB7248, Chapel Hill, NC 27599-7248. E-mail: knowles@med.unc.edu; or Maimoona A. Zariwala, Ph.D., 7007 Thurston-Bowles Building, CB7248, Chapel Hill, NC 27599-7248. E-mail: zariwala@med.unc.edu

This article has an online supplement, which is accessible from this issue's table of contents at www.atsjournals.org

Am J Respir Crit Care Med Vol 189, Iss 6, pp 707–717, Mar 15, 2014
Published 2014 by the American Thoracic Society
Originally Published in Press as DOI: 10.1164/rccm.201311-2047OC on February 25, 2014
Internet address: www.atsjournals.org

## Abstract

**Rationale:** Primary ciliary dyskinesia (PCD) is a genetically heterogeneous recessive disorder of motile cilia, but the genetic cause is not defined for all patients with PCD.

**Objectives:** To identify disease-causing mutations in novel genes, we performed exome sequencing, follow-up characterization, mutation scanning, and genotype-phenotype studies in patients with PCD.

**Methods:** Whole-exome sequencing was performed using NimbleGen capture and Illumina HiSeq sequencing. Sanger-based sequencing was used for mutation scanning, validation, and segregation analysis.

**Measurements and Main Results:** We performed exome sequencing on an affected sib-pair with normal ultrastructure in more than 85% of cilia. A homozygous splice-site mutation was detected in *RSPH1* in both siblings; parents were carriers. Screening *RSPH1* in 413 unrelated probands, including 325 with PCD and 88 with idiopathic bronchiectasis, revealed biallelic loss-of-function mutations in nine additional probands. Five affected siblings of probands in *RSPH1* families harbored the familial mutations. The 16 individuals with *RSPH1* mutations had some features of PCD; however, nasal nitric oxide levels were higher than in patients with PCD with other gene mutations (98.3 vs. 20.7 nl/min; $P < 0.0003$). Additionally, individuals with *RSPH1* mutations had a lower prevalence (8 of 16) of neonatal respiratory distress, and later onset of daily wet cough than typical for PCD, and better lung function ($FEV_1$), compared with 75 age- and sex-matched PCD cases (73.0 vs. 61.8, $FEV_1$ % predicted; $P = 0.043$). Cilia from individuals with *RSPH1* mutations had normal beat frequency (6.1 ± Hz at 25°C), but an abnormal, circular beat pattern.

**Conclusions:** The milder clinical disease and higher nasal nitric oxide in individuals with biallelic mutations in *RSPH1* provides evidence of a unique genotype-phenotype relationship in PCD, and suggests that mutations in *RSPH1* may be associated with residual ciliary function.


**Keywords:** cilia; Kartagener syndrome; ciliopathy; exome sequencing; RSPH1

### At a Glance Commentary

**Scientific Knowledge on the Subject:** Primary ciliary dyskinesia (PCD) is a rare genetically heterogeneous disorder that is associated with low levels of nasal nitric oxide and chronic otosinopulmonary disease. Pathogenic mutations in 28 genes can cause PCD, which accounts for approximately 70% of individuals affected with PCD.

**What This Study Adds to the Field:** This article describes mutation profiling of *RSPH1* in a large cohort of clinically well-characterized patients with PCD. Patients with PCD with mutations in *RSPH1* have milder respiratory disease and higher levels of nasal nitric oxide than seen in other "classic" forms of PCD.

Primary ciliary dyskinesia (PCD) (MIM 244400) is a genetically heterogeneous recessive disorder of motile cilia. Clinical manifestations (neonatal respiratory distress, early onset daily wet cough and nasal congestion, chronic otosinopulmonary disease, and male infertility) reflect abnormal cilia and flagellar function (1, 2). Dysfunction of specialized motile cilia at the ventral node during embryogenesis caused by mutations in many of the genes that cause PCD may lead to random organ placement, and approximately 50% of PCD affected individuals have organ laterality defects (1–3).

Mutations in 28 genes are known to cause PCD, and account for the genetic etiology in approximately 70% of affected individuals (1, 4–35). Most of these 28 genes result in defects in the ciliary axoneme, which can be defined by electron microscopic ultrastructural analysis (1). In the absence of clear structural defects, diagnosis of PCD remains challenging. Nasal nitric oxide (nNO) production, which is very low in patients with PCD with ciliary ultrastructural defects or mutations in *DNAH11* (mean ~21 nl/min), compared with normal subjects (~305 nl/min) (36), is being used as an aid to diagnosis. To date, there have been no reports of mutations in genes that cause PCD that are associated with a different (milder or more severe) PCD phenotype, compared with other PCD-causing gene mutations. To further explore genotype-phenotype relationships in PCD, we performed exome sequencing in two pediatric-aged siblings with a PCD-like clinical phenotype, but apparently normal ciliary ultrastructure and nNO values (~98 nl/min) that were not in the typical low range (~21 nl/min) for PCD. We identified biallelic mutations in *RSPH1* in the two affected siblings and performed follow-up testing for *RSPH1* mutations in a large number of other subjects with PCD or bronchiectasis of unknown cause. These studies defined a unique genotype-phenotype relationship for patients with PCD with mutations in *RSPH1*.

## Methods

### Protocol

We performed whole exome sequencing in two siblings with PCD-like phenotype, but normal ciliary ultrastructure and nondiagnostic nNO values. After identification of biallelic mutations in *RSPH1* in the probands, we tested for additional mutations in *RSPH1* in 413 unrelated individuals, including 117 PCD-affected probands with normal or nondiagnostic ciliary ultrastructure and nNO levels of less than 100 nl/min, 175 PCD-affected probands with outer dynein arm (ODA) ± inner dynein arm (IDA) defects or IDA ± microtubular disorganization, 33 PCD-affected probands without available ciliary ultrastructure, and 88 probands with idiopathic bronchiectasis and nNO greater than 100 nl/min.

### Genetic Testing

As previously described, exome sequencing was performed (NimbleGen v2 in-solution hybrid capture and Illumina HiSeq 2,000

sequencing) (37), sequences were aligned to the human reference genome (hg19) (38), single-nucleotide and insertion-deletion variants were called with GATK (39) (*see* Table E1 in the online supplement), SeattleSeq server was used for variant annotation, and common variants were filtered out (*see* Table E2) (11, 29, 37). Six genes had biallelic variants consistent with a recessive model and present in both affected siblings (*see* Tables E1 and E2). *RSPH1* was prioritized for validation (primer sequences in Table E3) by Sanger sequencing (Life Technologies, Carlsbad, CA) based on pathogenic potential, relevance of the gene to PCD, and analysis of large-scale coexpression datasets (11, 29, 40). On variant validation, segregation analysis was defined in parents and available family members of probands. Several methods were used to test for *RSPH1* mutations in 413 unrelated individuals (*see* Table E4), including Sanger-based high-throughput sequencing (RS&G Seattle; RC2-HL-10292) or at University of North Carolina (capillary electrophoresis), primer sequences in Table E3 (n = 71), additional whole-exome sequencing and targeted screening for *RSPH1* (n = 6), or a recently developed high throughput exon-sequencing technique (n = 336) (41).

### Analysis of Cilia Function

Freshly obtained nasal epithelia had analysis of ciliary movement and beat frequency, as reported (42). For *in vitro* studies, airway epithelia were expanded from nasal scrape biopsies using fibroblast conditioned media and Rho kinase inhibitor, Y-27632 (43). Cells were plated on porous filters and cultured at air-liquid interface until ciliary differentiation. High-speed videos (250 fps) were recorded (Nikon Eclipse TE-2000 inverted microscope [Nikon Instruments Inc., Melville, NY] and Roper ES-310T camera [Redlake MASD, Inc., San Diego, CA]), and ciliary beat frequency assessed (42). Waveform motion was analyzed by replaying the videos in slow motion and recording the positions of individual cilia.

### Statistical Analysis

Linear regression (age and sex as covariates) was used to compare lung function ($FEV_1$, % predicted) between 15 *RSPH1*-affected subjects and 75 age- and sex-matched non-*RSPH1* patients with PCD. A *t* test (unequal variance 1-trial) was used to compare nNO between 16 *RSPH1* patients and 149 patients with PCD with ciliary ultrastructural defects or mutations in *DNAH11* (36). Pair-wise *t* tests were used to compare ciliary motion (planar vs. rotational deviation from planar) between cultured ciliated cells from a clinically normal *RSPH1* carrier and two *RSPH1*-affected patients with PCD.

### Institutional Review Board Approval

The study was approved by the institutional review board for the Protection of the Rights of Human Subjects at the University of North Carolina and collaborating institutions. Written informed consent was obtained from study participants and/or their parents.

## Results

We identified a homozygous splice variant (c.275–2A>C) in *RSPH1* (RefSeq: NM_080860.2) in an affected sib-pair (#1444 [II-1]; #1774 [II-2]) who had normal ciliary ultrastructure in approximately 85% of their nasal cilia and nNO values approximately 90 nl/min (Table 1). Sanger sequencing confirmed inheritance *in trans* for these two siblings (Table 1; *see* Figure E1). Taken together, these data suggest mutations in *RSPH1* are likely the cause of PCD in this family.

We tested for mutations in *RSPH1* in 413 additional unrelated individuals and identified biallelic mutations in an additional 14 individuals (nine unrelated families) with PCD, but none in individuals with idiopathic bronchiectasis. Thus, biallelic mutations in *RSPH1* were found in a total of 10 families (16 individuals affected with PCD), and segregation analysis confirmed that the mutations were inherited *in trans* in the five families that could be tested, consistent with recessive inheritance (Table 1; *see* Figure E1). We also noted monoallelic mutations in three unrelated individuals. Despite *RSPH1* mutations in 13 unrelated kindreds, there were just four different putative mutations (Table 1, Figures 1 and E1), of which c.275–2A>C (disrupting a splice acceptor) represented 14 alleles (nine unrelated families); c.85G>T (p.Glu29*) represented six alleles (four unrelated families); c.407_410delAGTA (p.Lys136Metfs*6) represented two alleles (two unrelated families); and a single allele, c.287dupA (p.Asn96Lysfs*2) represented one individual. Two of the four putative mutant alleles (c.275–2A>C and c.85G>T) are in the single-nucleotide polymorphism database and exome variant server as rs151107532 and rs138320978, respectively. The minor allele frequencies in European Americans were low for both these variants (0.0011 minor allele frequencies [9 of 8,600] for c.275–2A>C and 0.0006 minor allele frequencies [5 of 8,600] for c.85G>T). Of the three putative mutant alleles that were observed in at least two unrelated families, haplotype analysis suggested these are founder mutations in individuals with Northern European ancestry (*see* Figure E2). In subjects from four families with homozygous mutations, parental DNA was unavailable. However, based on haplotype analysis, we conclude that these individuals likely carry homozygous mutations.

We noted monoallelic mutations in *RSPH1* in three additional families (n = 5 subjects) (*see* Table E5). One affected individual (#1473 [II-1]) also carried two disease-causing mutations in *DNAH5* (NM#001369.2) and had a ciliary ODA defect. In another family (#548), affected siblings were not concordant for the *RSPH1* mutation (*see* Table E5, Figure E1). Thus, it is very unlikely that *RSPH1* mutations are PCD-causing in these two families. In the third family (#552) with only one mutant allele, it is possible that there is another mutation that is undetected in *RSPH1* in the region that was not interrogated; alternatively, these individuals may have PCD-causing mutations in another gene. Thirteen benign variants were identified in this study (*see* Table E6).

To examine the functional significance of the c.275–2A>C splice site mutation, RNA was prepared from nasal epithelia obtained from two siblings (#1187 [II-1]; #1196 [II-2]) homozygous for the mutation. RNA was also isolated from an individual (#1371 [III-2]) compound heterozygous for c.275–2A>C and c.287dupA mutations and an unaffected mother (#1373 [II-2]) carrying c.275–2A>C mutation. Qualitative reverse-transcriptase polymerase chain reaction (RT-PCR) analysis using primers specific for exons 2 and 9 revealed a single major product of the expected size (930 bp) in RNA prepared from normal airway epithelia (Figure 2A). In contrast, RNA from the subject homozygous for the c.275–2A>C mutation produced primarily two shorter transcripts and several minor transcripts. One shorter (631 bp) transcript was caused by an out-of-frame deletion of exons 4–6 (r.275–573del [p.Glu93Lysfs*24]) and

**Table 1:** Demographic, Clinical Phenotype and Biallelic Mutations in *RSPH1* in 16 Subjects Affected with Primary Ciliary Dyskinesia from 10 Unrelated Families

| Family # | Subject # | Sex | Age (*yr*)* | Ethnicity | $FEV_1$ (*% Pred.*)† | nNO (*nl/min*)‡§ | Ciliary Ultrastructure "Normal" 9 + 2% | Situs Status | Neo RDS | Bxsis (*by CT Scan*) | Sinus Disease | Otitis Media | Fertility Status | Alleles | Location | Base Change | Amino Acid Change | Segregation‖ |
|---|---|---|---|---|---|---|---|---|---|---|---|---|---|---|---|---|---|---|
| Homozygous mutations | | | | | | | | | | | | | | | | | | |
| 398¶ | 1444 (II-1) | F | 14 | White | 88.3 | 91.4 | 84.0 | SS | Yes | Yes | No | Yes | Unknown | 1 | Intron 3 | c.275-2A>C | Aberrant splicing**‡ | Paternal |
| | | | | | | | | | | | | | | 2 | Intron 3 | c.275-2A>C | Aberrant splicing** | Maternal |
| 398¶ | 1774 (II-2) | F | 11 | White | 96.9 | 88.0 | 85.4 | SS | No | No | No | Yes | Unknown | 1 | Intron 3 | c.275-2A>C | Aberrant splicing** | Paternal |
| | | | | | | | | | | | | | | 2 | Intron 3 | c.275-2A>C | Aberrant splicing** | Maternal |
| 23¶ | 162 (II-1) | M | 52 | White | 68.2 | 48.7 | 83.3 | SS | No | Yes | Yes | Yes | Infertile | 1 | Intron 3 | c.275-2A>C | Aberrant splicing** | Paternal |
| | | | | | | | | | | | | | | 2 | Intron 3 | c.275-2A>C | Aberrant splicing** | Maternal |
| 23¶ | 163 (II-2) | F | 48 | White | 25.0 | 62.2 | 67.6 | SS | Yes | Yes | Yes | Yes | Unknown | 1 | Intron 3 | c.275-2A>C | Aberrant splicing** | Paternal |
| | | | | | | | | | | | | | | 2 | Intron 3 | c.275-2A>C | Aberrant splicing** | Maternal |
| 23¶ | 164 (II-3) | F | 44 | White | 37.5 | 90.5 | 83.3 | SS | No | Yes | Yes | No | Infertile | 1 | Intron 3 | c.275-2A>C | Aberrant splicing** | Paternal |
| | | | | | | | | | | | | | | 2 | Intron 3 | c.275-2A>C | Aberrant splicing** | Maternal |
| 265¶ | 1187 (II-1) | F | 52 | White | 63.3 | 112.2 | 86.2 | SS | No | Yes | Yes | No | Unknown | 1 | Intron 3 | c.275-2A>C | Aberrant splicing*‡ | NA |
| | | | | | | | | | | | | | | 2 | Intron 3 | c.275-2A>C | Aberrant splicing** | NA |
| 265¶ | 1196 (II-2) | M | 58 | White | 102.1 | 349.5 | 93.1 | SS | No | Yes | Yes | No | Infertile | 1 | Intron 3 | c.275-2A>C | Aberrant splicing** | NA |
| | | | | | | | | | | | | | | 2 | Intron 3 | c.275-2A>C | Aberrant splicing** | NA |
| 470 | 1571 (II-1) | M | 9 | White | 102.0 | 82.7 | NA | SS | Yes | Yes | No | No | Unknown | 1 | Intron 3 | c.275-2A>C | Aberrant splicing** | NA |
| | | | | | | | | | | | | | | 2 | Intron 3 | c.275-2A>C | Aberrant splicing** | NA |
| 494 | 1610 (II-1) | F | 48 | White | 76.0 | 121.8 | 77.6 | SS | No | Yes | Yes | No | Infertile | 1 | Intron 3 | c.275-2A>C | Aberrant splicing** | NA |
| | | | | | | | | | | | | | | 2 | Intron 3 | c.275-2A>C | Aberrant splicing** | NA |
| 663 | 2022 (II-1) | F | 40 | White | 96.0 | 43.5 | 63.4 | SS | Yes | Yes | Yes | Yes | Infertile | 1 | Exon 2 | c.85G>T | p.Glu29* | NA |
| | | | | | | | | | | | | | | 2 | Exon 2 | c.85G>T | p.Glu29* | NA |
| 347†† | 1331 (II-1) | F | 54 | White | 64.4 | 62.9 | 78.2 | SS | Yes | Yes | Yes | Yes | Infertile | 1 | Exon 2 | c.85G>T | p.Glu29* | Maternal |
| | | | | | | | | | | | | | | 2 | Exon 2 | c.85G>T | p.Glu29* | NA |
| Compound heterozygous mutations | | | | | | | | | | | | | | | | | | |
| 364¶ | 1370 (III-1) | M | 8 | White + Columbian | NA‡‡ | 30.4 | 71.6 | SS | Yes | Yes | Yes | Yes | Unknown | 1 | Intron 3 | c.275-2A>C | Aberrant splicing** | Maternal |
| | | | | | | | | | | | | | | 2 | Exon 4 | c.287dupA | p.Asn96Lysfs*2 | Paternal |
| 364¶ | 1371 (III-2) | F | 9 | White + Columbian | 54.0 | 88.4 | 85.0 | SS | Yes | Yes | Yes | Yes | Unknown | 1 | Intron 3 | c.275-2A>C | Aberrant splicing** | Maternal |
| | | | | | | | | | | | | | | 2 | Exon 4 | c.287dupA | p.Asn96Lysfs*2 | Paternal |
| 61¶ | 354 (II-1) | M | 20 | White | 93.6 | 106.0 | 85.0 | SS | No | Yes | Yes | Yes | Unknown | 1 | Intron 3 | c.275-2A>C | Aberrant splicing** | Paternal |
| | | | | | | | | | | | | | | 2 | Exon 5 | c.407_410delAGTA | p.Lys136Metfs*6 | Maternal |
| 61¶ | 355 (II-2) | F | 21 | White | 75.6 | 55.0 | 87.5 | SS | Yes | Yes | Yes | Yes | Unknown | 1 | Intron 3 | c.275-2A>C | Aberrant splicing** | Paternal |
| | | | | | | | | | | | | | | 2 | Exon 5 | c.407_410delAGTA | p.Lys136Metfs*6 | Maternal |
| 462 | 1562 (II-1) | M | 47 | White | 52.0 | 111.0 | 69.8 | SS | No | Yes | Yes | No | Infertile | 1 | Exon 2 | c.85G>T | p.Glu29* | NA |
| | | | | | | | | | | | | | | 2 | Exon 5 | c.407_410delAGTA | p.Lys136Metfs*6 | NA |

*Definition of abbreviations*: Bxsis = bronchiectasis; NA = not available; Neo RDS = neonatal respiratory distress in full-term neonates; nNO = nasal nitric oxide; SS = situs solitus.

*Age of most recently available spirometry.

†Lung function test ($FEV_1$% predicted).

‡For 16 affected individuals with biallelic mutations, there were 31 measurements of nNO; value listed for each subject equals mean of all measurements.

§Normal nNO levels are 304.6 ± 118.8 nl/min (mean ± SD), calculated from 78 healthy subjects (36).

‖Mutant allele shown to segregate with either the father's (paternal) or mother's (maternal) side of the family (pedigrees in Figure E1).

¶Affected siblings are listed under the same family numbers.

**Transcript analysis of c.275-2A>C (g.IVS3-2A>C) splice acceptor site mutation revealed aberrant splicing predicting aberrant protein (*see* details in Figures 1, E3, and E4).

††Parental consanguinity was noted.

‡‡Pulmonary resection in first day of life because of cystadenomatoid malformation, so unable to use lung function in comparison with classic PCD.

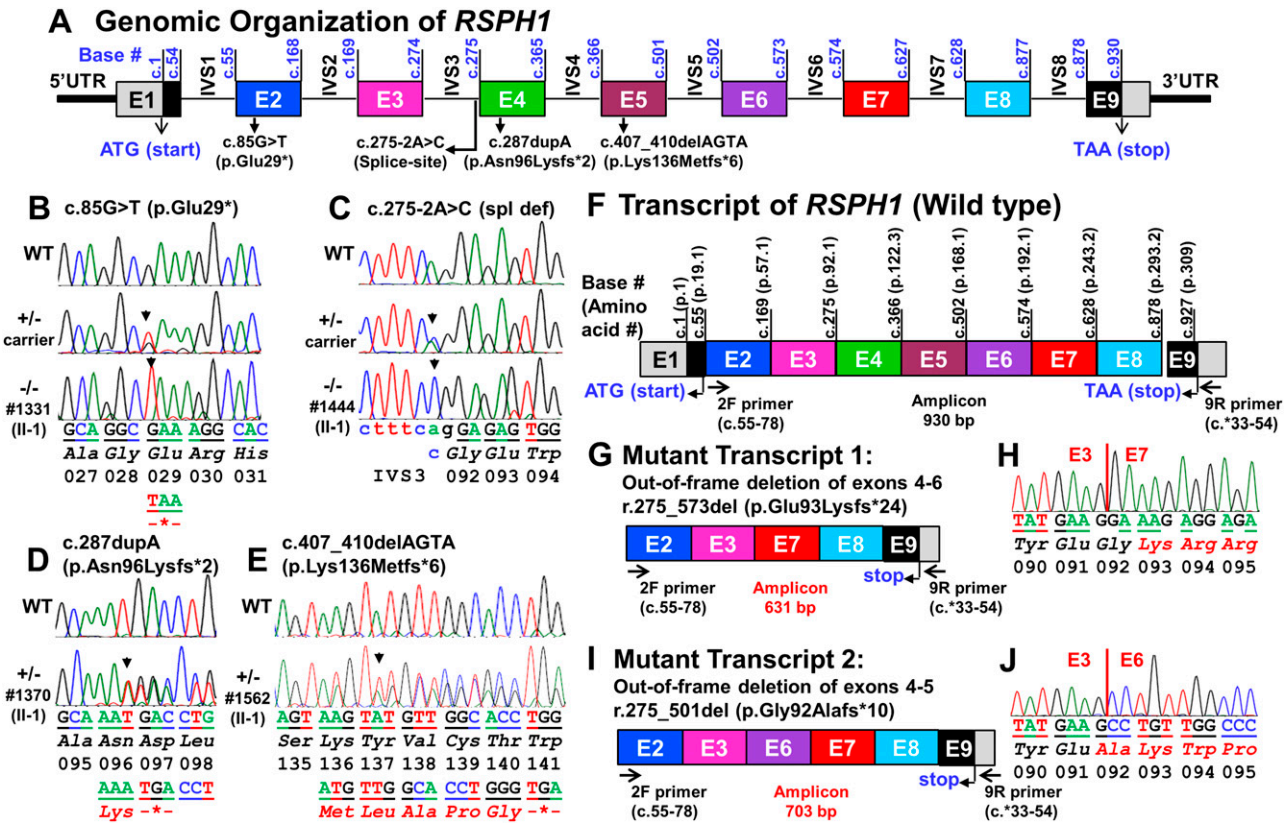


**Figure 1.** Genomic organization, location of primary ciliary dyskinesia (PCD)-causing mutations, and transcript analysis of RSPH1. (*A*) Schematic showing genomic organization of *RSPH1* (NM_080860.2), consisting of nine exons with 1,430 bp transcript, encoding 309 amino acids protein. *Solid box* designates exons "E," *horizontal lines* designates introns "IVS," and locations of 5′UTR, 3′UTR, start and stop codons are shown. Introns/exons are not drawn to scale. The positions of all four identified *RSPH1* putative mutations are indicated. (*B* and *C*) Homozygous (−/−) mutation in affected (*bottom*), heterozygous (+/−) carrier (*middle*), and corresponding wild-type (WT) sequences in control (*top*) for c.85G>T (p.Glu29*) and c.275–2A>C (splice acceptor site) mutations, respectively. (*D* and *E*) Heterozygous (+/−) mutation in affected (*bottom*) and corresponding WT sequences in control (*top*) for c.287dupA (p.Asn96Lysfs*2) and c.407_410delAGTA (p.Lys136Metfs*6) mutations, respectively. (*F*) Schematic showing WT transcripts of *RSPH1*. (*G–J*) Effect of homozygous c.275–2A>C splice acceptor site mutation from affected individual (#1187 [II-1]) was interrogated using reverse-transcriptase polymerase chain reaction with 2F+9R primers (*see* Table E3 for primer sequences). Two major transcripts and multiple minor transcripts were observed. (*G* and *H*) Major transcript 1 and 2 led to the out-of-frame deletion of exons 4–6 and exons 4 and 5, respectively, resulting in the premature translation termination signal. Schematic of the mutant transcripts and the corresponding electropherograms with exact location of the out-of-frame deletions are shown. Additional minor mutant transcripts are depicted in Figure E3. Forward and reverse primers are designated as "F" and "R," respectively, along with their cDNA locations, and amplicon sizes are shown in *red* fonts. Base sequence, amino acid sequence, and codon numbers are shown. Locations of the mutations are designate by an *arrow* and exon-exon junctions are shown by the *vertical solid red lines*. Further details with 2F+5R primer set are depicted in Figure E4.

another shorter (731 bp) transcript was caused by an out-of-frame deletion of exons 4–5 (r.275_501del [p.Gly92Alafs*10]), both leading to premature termination signals (Figure 1). The three minor products also represent aberrant transcripts (*see* Figure E3). Qualitative RT-PCR analysis of RNA from subject (#1187 [II-1]) homozygous for c.275–2A>C, using another primer set specific for exons 2–5, showed multiple aberrant transcripts (*see* Figure E3). RNA from the subject (#1371 [III-2]), compound heterozygous for mutations c.275–2A>C and c.287dupA, and an unaffected mother (#1373 [II-2]) who carried the c.275–2A>C mutation, was subjected to qualitative RT-PCR with exons 2–5 primers. A mixture of transcripts with apparently full-length products (either 417 bp for the wild-type transcript in the mother or 418 bp for the c.287dupA transcript in the affected subject) and a larger size (567 bp) transcript were obtained. The larger transcript was caused by the 150-bp insertion of intron 3 from the 3′end, causing a frameshift and resulting in premature termination (r.275–2A>C; r.275–1_275–150ins [p.Glu93Phefs*25]; data not shown). Western blotting of a total cell lysate prepared from nasal epithelia from a normal subject or from cultured human bronchial epithelial (HBE) cells revealed a strong RSPH1 signal, whereas no signal was detected in nasal epithelia from a subject affected with PCD (#1370 [III-1]) harboring compound heterozygous mutations (c.275–2A>C and c.287dupA) (Figure 2B).

To investigate the expression of *RSPH1* in ciliated cells, HBE cells were cultured at air-liquid interface and RNA was isolated at different times during differentiation (44). Figure 3A shows that *RSPH1* was not expressed early in culture (Days 4 and 8), but was strongly expressed thereafter. This pattern parallels the expression of dynein

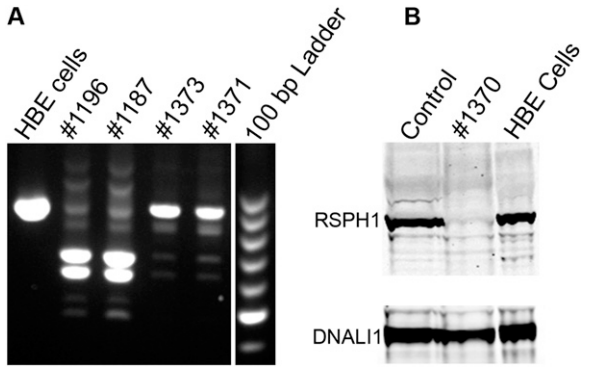


**Figure 2.** Effect of the c.275–2A>C splice site mutation on RSPH1 expression *in vivo*. (*A*) RNA was prepared from cultured human bronchial epithelial (HBE) cells from a normal subject and nasal scrape biopsies from individuals with primary ciliary dyskinesia (PCD) (#1196 [II-2], #1187 [II-1]) with homozygous splice site (c.275–2A>C) mutations, a carrier (#1373 [II-2]) with one splice site (c.275–2A>C) mutation, and an individual (#1371 [III-2]) with a splice site (c.275–2A>C) and a frameshift (c.287dupA) compound heterozygous mutations. Reverse-transcriptase polymerase chain reaction of the control sample resulted in a single, full-length product of approximately 930 bp, whereas the c.275–2A>C mutation resulted in predominantly two smaller products of approximately 650 and 750 bp, along with multiple other aberrantly spliced products (*brightest fragment* on ladder represents 500 bp). Heterozygous individuals generated a mixture of the full-length and aberrant products. Extra lanes between the samples and the marker lane were removed from the image, as indicated by the *white line*. (*B*) Western blot of total protein from a normal control nasal biopsy, a PCD subject (#1370 [III-1]) with a splice site (c.275–2A>C) and a frameshift (c.287dupA) compound heterozygous mutations, and cultured (normal) HBE cells. The PCD sample shows no clear signal for RSPH1. The blot was reprobed with an antibody against DNALI1 to demonstrate the presence of approximately equal numbers of cilia between samples.

axonemal intermediate chain 1 (*DNAI1* [NM_012144.2]), another gene in which mutations cause PCD (24, 30), which suggests *RSPH1* plays a specific role in ciliated cells. In our studies, RSPH1 was not detected by Western blot in lysates of undifferentiated HBE cells, whereas a clear signal was present in lysates of differentiated (ciliated) cultures, in agreement with the RNA data (Figure 3B). A strong signal for RSPH1 was also observed in detergent isolated axonemes, demonstrating that the RSPH1 protein is an integral part of the ciliary axoneme. Immunocytochemistry of HBE cells showed that the RSPH1 antibody reacted with the cilia (Figure 3C), whereas no signal was observed with control IgG, further confirming the ciliary location of RSPH1. Taken together, these studies demonstrate that RSPH1 is expressed during ciliated cell differentiation, is an integral protein of the axoneme, and mutations in *RSPH1* can be PCD-causing.

The clinical manifestations of otosinopulmonary disease in our subjects with biallelic mutations in *RSPH1* resembled those in individuals with classic PCD with dynein arm defects, because all subjects developed bronchiectasis by their mid-late teenage years (Table 1), and most had recurrent otitis media and sinusitis starting in childhood. However, the prevalence of neonatal respiratory distress was lower (50%) than seen in classic PCD (75–85%), and only two subjects were reported to have an onset of daily year-round wet cough within the first year of life that characterizes 75–85% of cases with classic PCD (1). To assess severity of the lung disease in individuals with biallelic *RSPH1* mutations, we compared their lung function ($FEV_1$% predicted) with individuals defined by ultrastructural defects and/or biallelic PCD-causing mutations in other (non-*RSPH1*) genes (45). One of our 16 cases with biallelic mutations in *RSPH1* could not be used for this comparison of lung function, because a cystadenomatoid lung malformation required pulmonary resection within the first 24 hours after birth. The other 15 cases with biallelic mutations in *RSPH1* were

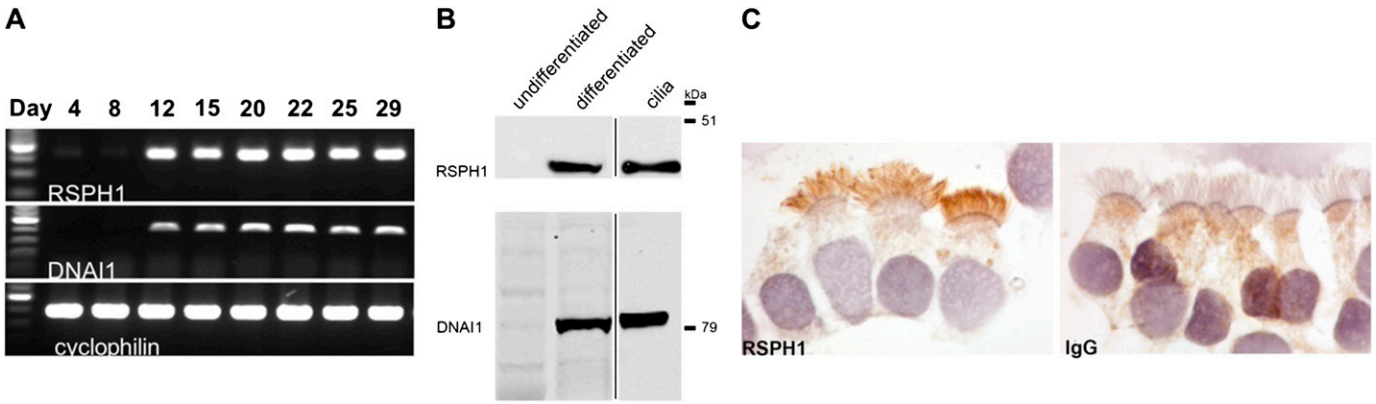


**Figure 3.** Expression of RSPH1 in cultured human bronchial epithelial (HBE) cells. (*A*) Control HBE cells were cultured at an air-liquid interface for the indicated time and total RNA was isolated (44). Reverse-transcriptase polymerase chain reaction with specific primers demonstrates that *RSPH1* and *DNAI1* (NM_012144.2) are not expressed in early, undifferentiated cultures, but are induced during ciliated cell differentiation. *Cyclophilin A* (*PPIA*) (NM_021130.3) expression (positive control) does not change over time. (*B*) Western blot of total cell lysates from undifferentiated and differentiated HBE cells and isolated ciliary axonemes (50). *RSPH1* is not detected in the undifferentiated cells, but is present in the differentiated cell lysates and in the isolated ciliary axonemes. Extra lanes between the samples were removed from the image, as indicated by the black line. Two separate Western blots were probed with RSPH1 (*top*) and DNAI1 (*bottom*). (*C*) Cultured HBE cells were immunostained with a monoclonal antibody against RSPH1 or with control IgG. The RSPH1 antibody clearly reacts with the cilia, confirming the presence of RSPH1 in the axoneme.

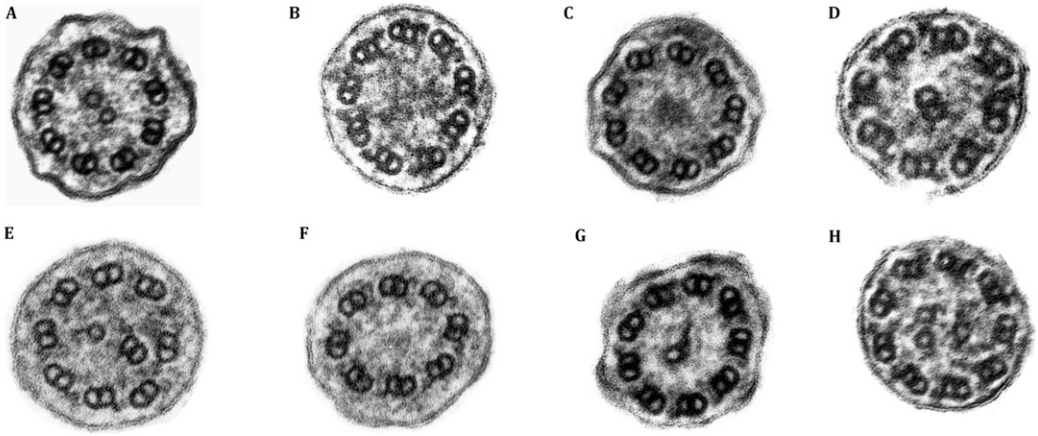


| | (A) Normal Axonemal Structure | Absence of Central Pair (B) or Electron Dense Material (C) | Translocation of Outer Doublet to Cilia (D) Center or Other Site (E) or Other Changes (e.g., 8+0) (F) | (G) Single Microtubule in Center | (H) Off-Center Central Pair |
|---|---|---|---|---|---|
| Mean | 80.1% | 12.1% | 5.1% | 1.4% | 1.2% |
| Range | 63.4 – 93.1% | 0 - 24.7% | 3.0 – 14.1% | 0 – 5.9 % | 0 – 6.9% |

**Figure 4.** Electron micrographic findings. A total of 756 ciliary cross-sections were scored from 15 subjects affected with primary ciliary dyskinesia (PCD) with biallelic mutations in *RSPH1*, and representative images are shown. (*A*) Normal (9 + 2) axonemal structure including outer doublet and the central apparatus (80.1% of cilia images). (*B* and *C*) Complete absence of the central apparatus (9 + 0), or electron-dense material in central area (12.1% of cilia images). (*D–F*) Translocation of outer doublet to either replace central pair or into the central region (8 + 1) with extra singlet microtubule, or other abnormalities including eight outer doublets without normal central apparatus (8 + 0) (5.1% of cilia images). (*G*) A single microtubule in the center instead of central pair (9 + 1) (1.4% of cilia images). (*H*) Off-center central pair with extra singlet (1.2% of cilia images).

compared with 75 age- and sex-matched individuals with classic PCD, using linear regression (age and sex as covariates). The $FEV_1$ (% predicted) was better in *RSPH1* cases by approximately 11% (73.0 vs. 61.8, % predicted; $P = 0.043$) (*see* Table E7), which is congruent with less prominent respiratory symptoms early in life in *RSPH1* patients. We also noted that $FEV_1$ was better (~11%) in 15 *RSPH1* cases when we restricted age and gender matching (1:3) to 45 subjects with dynein arm defects (ODA and ODA + IDA) (*see* subscript to Table E7).

Another striking difference in the phenotype of subjects with mutations in *RSPH1* was a higher level of nNO production than has been previously reported for mutations in any of the other PCD-causing genes, including *DNAH11*, which is associated with normal ciliary ultrastructure (1, 10). The mean nNO in 149 prospectively studied PCD cases with ciliary ultrastructural defects or mutations in *DNAH11* was 20.7 nl/min (36), whereas the mean nNO value in our 16 subjects with *RSPH1* mutations was nearly fivefold higher (98.3 nl/min; $P < 0.0003$). Indeed, 10 of these 16 *RSPH1* individuals had nNO values that were above the disease-specific cutoff value (77 nl/min) that we recently established in 149 individuals affected with PCD versus 78 healthy subjects and 146 disease-controls (36).

Quantitative ultrastructural analysis of 756 cilia from 15 subjects with biallelic mutations in *RSPH1* showed that 80.1 ± 8.4% (mean ± SD) of the cilia had a normal 9 + 2 and dynein arm ultrastructure, although radial spokes were not well seen (Figure 4). The percentage of cilia from *RSPH1* patients with normal ultrastructure is lower than seen in normal subjects in our hands (92.6 ± 6.1%, data not shown) and the study by Papon and coworkers (95%) (46). In the cilia from *RSPH1* subjects with clear-cut defects, the most common abnormalities were absence of the central pair (~12%) and translocation of an outer doublet into the central region (~5%) with or without a central pair being present (Figure 4). However, the percentage of cilia with normal ultrastructure in individuals with biallelic mutations in *RSPH1* ranges from 63.4% to 93.1%, which overlaps with the range (80–100%) from the control individuals (46); indeed, less than half (7 of 16) of the subjects with *RSPH1* mutations had more central apparatus defects than the lower range reported in cilia from normal subjects (46).

We assessed ciliary waveform by high-speed video microscopy in freshly obtained nasal epithelia from nine subjects with biallelic mutations in *RSPH1*, and measured ciliary beat frequency (Sisson-Ammons Video Analysis; room temperature) in samples from four of these subjects (42). The mean ciliary beat frequency (6.1 ± 1.7 Hz) was only slightly lower than normal (7.3 ± 1.5 Hz) from multiple measurements in 10 random fields (42). When cilia were viewed from a lateral perspective (*see* Videos E1 and E2), the *RSPH1* cilia showed vigorous activity, but a slightly reduced range of motion compared with normal, and some fields showed mild dyskinesia (poorly coordinated movement) with adjacent cilia. When viewed from above (*see* Videos E3 and E4), the cilia exhibited rotational (clockwise) movement (for control, *see* Video E5).

To examine the effect of mutations in *RSPH1* on ciliary function in the absence of infection and inflammation, ciliary motion of cultured epithelia was analyzed by replaying high-speed videos in slow motion and recording the positions of individual cilia. For each sample, three to five cilia from three separate cells were tracked over

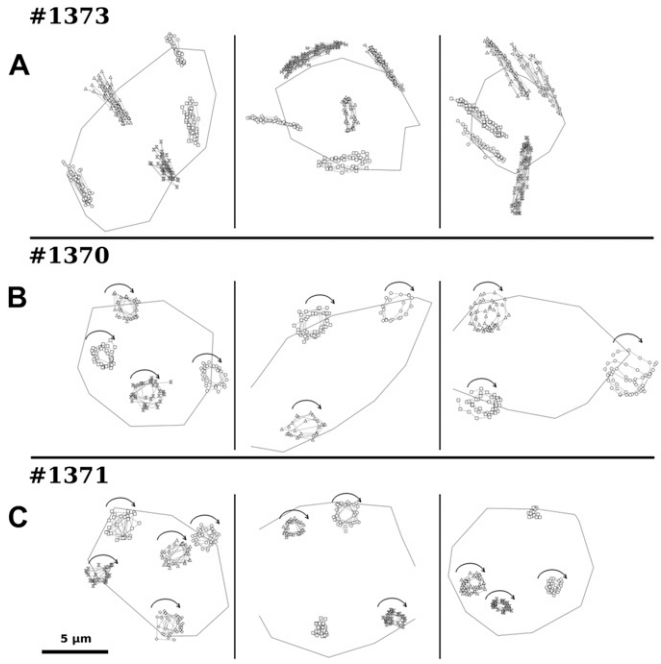


**Figure 5.** Mutations in RSPH1 result in a circular wave form. (*A*) Nasal epithelial cells from a heterozygous carrier mother (#1373 [II-2]), and (*B* and *C*) two affected children (#1370 [III-1] and #1371 [III-2]) were expanded in culture (43) and allowed to differentiate at the air-liquid interface (44). High-speed videos were recorded from above the cultures and analyzed in slow motion (*see* Videos E6–E8). (*A*) The cilia on three individual cells from the carrier mother (#1373 [II-2]) beat in a mostly planar (back and forth) direction. (*B* and *C*) The cilia on three individual cells from each of the children affected with primary ciliary dyskinesia (PCD) (#1370 [III-1] and #1371 [III-2]) moved in a clockwise circle when viewed from above. To compare the ciliary activity quantitatively, a line of best fit was determined for each cilia track. The mean distance ($d_{mean}$) of the cilium from that line and the maximum distance ($d_{max}$) from the centroid along that line were calculated. The $d_{mean}$ values (micrometers, ± SD) were 0.27 ± 0.26 (n = 15) for the mother (#1373 [II-2]) but much greater for children affected with PCD (#1370 [III-1], 0.53 ± 0.10 [n = 10]; #1371 [III-2], 0.36 ± 0.13 [n = 13]). The ratio of these values ($r = d_{mean} / d_{max}$) gives a measure of the ciliary beat shape with a lower value denoting a straighter, more planar, beat. The *r* values for the PCD cells (#1370 [III-1], 0.35 ± 0.068; #1371 [III-2], 0.36 ± 0.085) were significantly different than those of the carrier mother (#1373 [II-2], 0.11 ± 0.08; $P < 6.4 \times 10^{8}$), reflecting the defective ciliary activity.

several cycles. Cilia from the clinically unaffected (heterozygous carrier) mother (#1373 [II-2]) beat in a mostly planar (back and forth) motion, whereas cilia from the affected siblings (#1370 [III-1] and #1371 [III-2]) moved in a circular pattern (Figure 5). When viewed from above, the cilia exhibited rotational (clockwise) movement, similar to the rotational movement of nodal (9 + 0) cilia (47). Quantitative analysis (Figure 5) demonstrated that the rotational waveform of cilia from two siblings with biallelic mutations in *RSPH1* was different from the planar waveform of cilia from the carrier mother (#1373 [II-2]) ($P < 6.4 \times 10^{8}$). Thus, although mutations in *RSPH1* do not greatly reduce ciliary activity, the ciliary waveform is altered (Figure 5; *see* Videos E6–E8).

## Discussion

PCD is a genetically heterogeneous, autosomal-recessive disorder; indeed, mutations in 28 genes have been reported to cause PCD (1, 4–35). However, there has been no previous report of any unique genotype-phenotype association in PCD. This study of patients with biallelic mutations in *RSPH1* is the first to demonstrate an association between loss-of-function mutations in a PCD-causing gene and a milder clinical phenotype and higher levels of nNO, as compared with patients with PCD with typical ultrastructural defects or mutations in genes that are commonly associated with PCD.

Our discovery of mutations in *RSPH1* as PCD-causing is congruent with the recent report of *RSPH1* mutations in PCD by Kott and coworkers (35), although that study did not discuss any genotype-phenotype associations. The discovery of *RSPH1* as a PCD-causing gene is also congruent with what is known about the protein product of *RSPH1*. Radial spoke head 1 homolog (RSPH1; 309 amino-acids; NP_543136) is approximately 40% identical to the *Chlamydomonas* radial spoke protein 1 (RSP1; 814 amino-acids; XP_001693353), a component of the radial spoke head in flagellar axonemes (Figure 1) (48). Although there are no *Chlamydomonas RSP1* mutant strains available, strains that are missing the radial spoke head because of mutations in *RSP4*, *RSP6*, or *RSP9* all show obvious motility defects. Human *RSPH1* contains six membrane occupation and recognition nexus domains, which regulate intracellular $Ca^{2+}$ signaling (49).

Our studies showing expression of *RSPH1* during differentiation of ciliated airway epithelia, and the presence of RSPH1 in detergent isolated axonemes of normal cilia, demonstrate that *RSPH1* has a role in ciliated cells, and is an integral protein of the ciliary axonemes. These data are consistent with recent immunoelectron microscopic studies that have localized RSPH1 to the radial spoke region of the sperm flagellum, and immunofluorescence studies that show localization of RSPH1 to the cilia of epithelia in the trachea and ependyma (35, 49).

Because *RSPH1* mutant respiratory cilia have intact dynein arms, ciliary velocity is not very affected by the radial spoke mutations. Our studies clearly document that *RSPH1* mutant cilia have a clockwise rotational movement when viewed from above, and the waveform approximates the circular movement of nodal cilia, which lacks the central apparatus (47). Others have reported that ciliary motility in PCD-affected individuals harboring mutations in radial spoke head genes (*RSPH4A* and *RSPH9*) resembles the rotary movement of nodal (9 + 0) cilia (6).

It is noteworthy that all 16 individuals with biallelic mutations in *RSPH1*, including the nine with homozygous splice site variants, had situs solitus (Table 1). This is congruent with reports of other patients with PCD who have radial spoke head mutations in *RSPH4A* (NM_152732.4) and

*RSPH9* (NM_001010892.2) (6, 32, 35). The lack of laterality defects is consistent with the recognition that the 9 + 0 embryologic nodal cilium does not contain radial spokes and is unaffected by central apparatus defects; therefore, normal organ lateralization is preserved during embryogenesis.

The findings of our study have important implications for PCD, particularly as relates to genotype and phenotype. First, three of the four mutations we describe were included in the recent report by Kott and coworkers (35). Our haplotype analysis demonstrated that three of these mutations are likely to be founder mutations in individuals with Northern European ancestry (*see* Figure E2). The data in Kott and coworkers are consistent with this interpretation, but they did not provide any haplotype analysis (35). Second, our in-depth analysis of the clinical and ciliary phenotype of individuals with *RSPH1* mutations indicates that they have milder respiratory disease than PCD individuals with mutations in other published genes, including *DNAH11*, which is associated with normal ciliary ultrastructure; specifically, individuals with *RSPH1* mutations had a lower incidence of neonatal respiratory distress, a later onset of daily year round wet cough, better lung function, and significantly higher levels of nNO. Our results are consistent with those of Kott and coworkers (35), who reported that only 4 of the 12 subjects they studied had neonatal respiratory distress, whereas two of their four subjects with data had nNO levels greater than 77 nl/min, which is the disease-specific cutoff in PCD (36). Third, although the mechanism responsible for the milder phenotype and higher nNO values is unknown, waveform analysis that we performed in nasal epithelial cells cultured in the absence of infection and inflammation demonstrated that *RSPH1* mutant cilia beat with an almost normal frequency, but with a circular waveform similar to that reported for mutations in two other radial spoke genes, *RSPH4A* and *RSPH9* (6, 32). However, patients with mutations in *RSPH4A* and *RSPH9* seem to have a typical PCD phenotype (6, 32), including low nNO values (average, 14.2 nl/min; range, 5.9–22.6 nl/min; n = 8) (6, 32). We speculate that *RSPH1* mutant cilia may have some residual functional activity to stimulate nitric oxide synthases in the ciliated cell apical membrane, and produce more nitric oxide than individuals with classic PCD (1). Fourth, the higher level of nNO in *RSPH1* individuals is of particular importance, because nNO is being used to assist with screening and diagnosing PCD in subjects without clear-cut ciliary ultrastructure defects. Because approximately 50% of the subjects with PCD in our study had normal ultrastructure in more than 80% of their cilia, the higher levels of nNO and milder disease phenotype makes it challenging to confirm a correct diagnosis, unless genetic testing is performed. Finally, it is likely that mutations in other genes will be identified that result in higher nNO and a milder PCD phenotype; however, these cases are not currently recognized and will likely require discovery and confirmation by genetic testing. Ultimately, the identification of additional mutations in novel genes that cause PCD, and implementation of genetic testing, will result in improved diagnosis, clinical care, and outcomes in affected individuals. ■

**Author disclosures** are available with the text of this article at www.atsjournals.org.

**Acknowledgment:** The authors thank PCD subjects and family members, and Ms. Michele Manion (founder of the US PCD Foundation). They acknowledge other investigators and coordinators of the Genetic Disorders of Mucociliary Clearance Consortium, including Ms. Andrea Henkel (National Institute of Allergy and Infectious Diseases, Bethesda, MD), Dr. Jeffrey Atkinson and Ms. Jane Quante (Washington University in St. Louis, St. Louis, MO), Ms. Shelley Mann (The Children's Hospital, Aurora, CO), Ms. Molly Elliott (Children's Hospital and Regional Medical Center, Seattle, WA), Ms. Jacquelyn Zirbes (Stanford University Medical Center, Palo Alto, CA), Dr. Christopher Czaja and Ms. Adrah Levin (National Jewish Health, Denver, CO) Ms. Melody Miki (The Hospital for Sick Children, Toronto, Ontario, Canada), and Ms. Susan Minnix and Ms. Caroline LaFave-O'Connor (University of North Carolina at Chapel Hill, Chapel Hill, NC). The authors also acknowledge the other investigators and coordinators of the NHLBI GO Exome Sequencing Project and Family Studies Project Team. They also thank Dr. Jaclyn Stonebraker, Ms. Lu Huang, Ms. Kimberly Burns, and Ms. Rhonda Pace from University of North Carolina for technical assistance; Ms. Elizabeth Godwin, for administrative support; and Ms. Syanne Olson for manuscript preparation. The authors thank the NIH-NHLBI GO Exome Sequencing Project and its ongoing studies that produced and provided exome variant calls for comparison: the Lung GO Sequencing Project (HL-102923), the WHI Sequencing Project (HL-102924), the Heart GO Sequencing Project (HL-103010), the Broad GO Sequencing Project (HL-102925), the Seattle GO Sequencing Project (HL-102926), and the Family Studies Project Team.

## References

1. Knowles MR, Daniels LA, Davis SD, Zariwala MA, Leigh MW. Primary ciliary dyskinesia. Recent advances in diagnostics, genetics, and characterization of clinical disease. *Am J Respir Crit Care Med* 2013; 188:913–922.
2. Leigh MW, Pittman JE, Carson JL, Ferkol TW, Dell SD, Davis SD, Knowles MR, Zariwala MA. Clinical and genetic aspects of primary ciliary dyskinesia/Kartagener syndrome. *Genet Med* 2009;11:473–487.
3. Zariwala MA, Knowles MR, Omran H. Genetic defects in ciliary structure and function. *Annu Rev Physiol* 2007;69:423–450.
4. Bartoloni L, Blouin JL, Pan Y, Gehrig C, Maiti AK, Scamuffa N, Rossier C, Jorissen M, Armengot M, Meeks M, *et al*. Mutations in the *DNAH11* (axonemal heavy chain dynein type 11) gene cause one form of situs inversus totalis and most likely primary ciliary dyskinesia. *Proc Natl Acad Sci USA* 2002;99:10282–10286.
5. Becker-Heck A, Zohn IE, Okabe N, Pollock A, Lenhart KB, Sullivan-Brown J, McSheene J, Loges NT, Olbrich H, Haeffner K, *et al*. The coiled-coil domain containing protein CCDC40 is essential for motile cilia function and left-right axis formation. *Nat Genet* 2011;43:79–84.
6. Castleman VH, Romio L, Chodhari R, Hirst RA, de Castro SC, Parker KA, Ybot-Gonzalez P, Emes RD, Wilson SW, Wallis C, *et al*. Mutations in radial spoke head protein genes *RSPH9* and *RSPH4A* cause primary ciliary dyskinesia with central-microtubular-pair abnormalities. *Am J Hum Genet* 2009;84:197–209.
7. Duquesnoy P, Escudier E, Vincensini L, Freshour J, Bridoux AM, Coste A, Deschildre A, de Blic J, Legendre M, Montantin G, *et al*. Loss-of-function mutations in the human ortholog of Chlamydomonas reinhardtii ODA7 disrupt dynein arm assembly and cause primary ciliary dyskinesia. *Am J Hum Genet* 2009;85:890–896.
8. Hjeij R, Lindstrand A, Francis R, Zariwala MA, Liu X, Li Y, Damerla R, Dougherty GW, Abouhamed M, Olbrich H, *et al*. *ARMC4* mutations cause primary ciliary dyskinesia with randomization of left/right body asymmetry. *Am J Hum Genet* 2013;93:357–367.
9. Horani A, Druley TE, Zariwala MA, Patel AC, Levinson BT, Van Arendonk LG, Thornton KC, Giacalone JC, Albee AJ, Wilson KS, *et al*. Whole-exome capture and sequencing identifies *HEATR2* mutation as a cause of primary ciliary dyskinesia. *Am J Hum Genet* 2012;91:685–693.
10. Knowles MR, Leigh MW, Carson JL, Davis SD, Dell SD, Ferkol TW, Olivier KN, Sagel SD, Rosenfeld M, Burns KA, *et al*.; Genetic

Disorders of Mucociliary Clearance Consortium. Mutations of *DNAH11* in patients with primary ciliary dyskinesia with normal ciliary ultrastructure. *Thorax* 2012;67:433–441.
11. Knowles MR, Leigh MW, Ostrowski LE, Huang L, Carson JL, Hazucha MJ, Yin W, Berg JS, Davis SD, Dell SD, *et al*.; Genetic Disorders of Mucociliary Clearance Consortium. Exome sequencing identifies mutations in *CCDC114* as a cause of primary ciliary dyskinesia. *Am J Hum Genet* 2013;92:99–106.
12. Kott E, Duquesnoy P, Copin B, Legendre M, Dastot-Le Moal F, Montantin G, Jeanson L, Tamalet A, Papon JF, Siffroi JP, *et al*. Loss-of-function mutations in *LRRC6*, a gene essential for proper axonemal assembly of inner and outer dynein arms, cause primary ciliary dyskinesia. *Am J Hum Genet* 2012;91:958–964.
13. Loges NT, Olbrich H, Fenske L, Mussaffi H, Horvath J, Fliegauf M, Kuhl H, Baktai G, Peterffy E, Chodhari R, *et al*. *DNAI2* mutations cause primary ciliary dyskinesia with defects in the outer dynein arm. *Am J Hum Genet* 2008;83:547–558.
14. Loges NT, Olbrich H, Becker-Heck A, Häffner K, Heer A, Reinhard C, Schmidts M, Kispert A, Zariwala MA, Leigh MW, *et al*. Deletions and point mutations of *LRRC50* cause primary ciliary dyskinesia due to dynein arm defects. *Am J Hum Genet* 2009;85:883–889.
15. Mazor M, Alkrinawi S, Chalifa-Caspi V, Manor E, Sheffield VC, Aviram M, Parvari R. Primary ciliary dyskinesia caused by homozygous mutation in *DNAL1*, encoding dynein light chain 1. *Am J Hum Genet* 2011;88:599–607.
16. Merveille AC, Davis EE, Becker-Heck A, Legendre M, Amirav I, Bataille G, Belmont J, Beydon N, Billen F, Clément A, *et al*. *CCDC39* is required for assembly of inner dynein arms and the dynein regulatory complex and for normal ciliary motility in humans and dogs. *Nat Genet* 2011;43:72–78.
17. Mitchison HM, Schmidts M, Loges NT, Freshour J, Dritsoula A, Hirst RA, O'Callaghan C, Blau H, Al Dabbagh M, Olbrich H, *et al*. Mutations in axonemal dynein assembly factor *DNAAF3* cause primary ciliary dyskinesia. *Nat Genet* 2012;44:381–389, S1–S2.
18. Moore DJ, Onoufriadis A, Shoemark A, Simpson MA, zur Lage PI, de Castro SC, Bartoloni L, Gallone G, Petridi S, Woollard WJ, *et al*. Mutations in *ZMYND10*, a gene essential for proper axonemal assembly of inner and outer dynein arms in humans and flies, cause primary ciliary dyskinesia. *Am J Hum Genet* 2013;93:346–356.
19. Olbrich H, Häffner K, Kispert A, Völkel A, Volz A, Sasmaz G, Reinhardt R, Hennig S, Lehrach H, Konietzko N, *et al*. Mutations in *DNAH5* cause primary ciliary dyskinesia and randomization of left-right asymmetry. *Nat Genet* 2002;30:143–144.
20. Olbrich H, Schmidts M, Werner C, Onoufriadis A, Loges NT, Raidt J, Banki NF, Shoemark A, Burgoyne T, Al Turki S, *et al*.; UK10K Consortium. Recessive *HYDIN* mutations cause primary ciliary dyskinesia without randomization of left-right body asymmetry. *Am J Hum Genet* 2012;91:672–684.
21. Omran H, Kobayashi D, Olbrich H, Tsukahara T, Loges NT, Hagiwara H, Zhang Q, Leblond G, O'Toole E, Hara C, *et al*. Ktu/PF13 is required for cytoplasmic pre-assembly of axonemal dyneins. *Nature* 2008; 456:611–616.
22. Onoufriadis A, Paff T, Antony D, Shoemark A, Micha D, Kuyt B, Schmidts M, Petridi S, Dankert-Roelse JE, Haarman EG, *et al*.; UK10K. Splice-site mutations in the axonemal outer dynein arm docking complex gene *CCDC114* cause primary ciliary dyskinesia. *Am J Hum Genet* 2013;92:88–98.
23. Panizzi JR, Becker-Heck A, Castleman VH, Al-Mutairi DA, Liu Y, Loges NT, Pathak N, Austin-Tse C, Sheridan E, Schmidts M, *et al*. *CCDC103* mutations cause primary ciliary dyskinesia by disrupting assembly of ciliary dynein arms. *Nat Genet* 2012;44:714–719.
24. Pennarun G, Escudier E, Chapelin C, Bridoux AM, Cacheux V, Roger G, Clément A, Goossens M, Amselem S, Duriez B. Loss-of-function mutations in a human gene related to *Chlamydomonas reinhardtii* dynein IC78 result in primary ciliary dyskinesia. *Am J Hum Genet* 1999;65:1508–1519.
25. Tarkar A, Loges NT, Slagle CE, Francis R, Dougherty GW, Tamayo JV, Shook B, Cantino M, Schwartz D, Jahnke C, *et al*.; UK10K. DYX1C1 is required for axonemal dynein assembly and ciliary motility. *Nat Genet* 2013;45:995–1003.
26. Wirschell M, Olbrich H, Werner C, Tritschler D, Bower R, Sale WS, Loges NT, Pennekamp P, Lindberg S, Stenram U, *et al*. The nexin-dynein regulatory complex subunit DRC1 is essential for motile cilia function in algae and humans. *Nat Genet* 2013;45: 262–268.
27. Zariwala MA, Gee HY, Kurkowiak M, Al-Mutairi DA, Leigh MW, Hurd TW, Hjeij R, Dell SD, Chaki M, Dougherty GW, *et al*. *ZMYND10* is mutated in primary ciliary dyskinesia and interacts with LRRC6. *Am J Hum Genet* 2013;93:336–345.
28. Horani A, Brody SL, Ferkol TW, Shoseyov D, Wasserman MG, Ta-shma A, Wilson KS, Bayly PV, Amirav I, Cohen-Cymberknoh M, *et al*. *CCDC65* mutation causes primary ciliary dyskinesia with normal ultrastructure and hyperkinetic cilia. *PLoS ONE* 2013;8: e72299.
29. Knowles MR, Ostrowski LE, Loges NT, Hurd T, Leigh MW, Huang L, Wolf WE, Carson JL, Hazucha MJ, Yin W, *et al*. Mutations in *SPAG1* cause primary ciliary dyskinesia associated with defective outer and inner dynein arms. *Am J Hum Genet* 2013;93:711–720.
30. Zariwala MA, Leigh MW, Ceppa F, Kennedy MP, Noone PG, Carson JL, Hazucha MJ, Lori A, Horvath J, Olbrich H, *et al*. Mutations of *DNAI1* in primary ciliary dyskinesia: evidence of founder effect in a common mutation. *Am J Respir Crit Care Med* 2006;174:858–866.
31. Hornef N, Olbrich H, Horvath J, Zariwala MA, Fliegauf M, Loges NT, Wildhaber J, Noone PG, Kennedy M, Antonarakis SE, *et al*. *DNAH5* mutations are a common cause of primary ciliary dyskinesia with outer dynein arm defects. *Am J Respir Crit Care Med* 2006;174: 120–126.
32. Daniels ML, Leigh MW, Davis SD, Armstrong MC, Carson JL, Hazucha M, Dell SD, Eriksson M, Collins FS, Knowles MR, *et al*. Founder mutation in *RSPH4A* identified in patients of Hispanic descent with primary ciliary dyskinesia. *Hum Mutat* 2013;34:1352–1356.
33. Antony D, Becker-Heck A, Zariwala MA, Schmidts M, Onoufriadis A, Forouhan M, Wilson R, Taylor-Cox T, Dewar A, Jackson C, *et al*. Mutations in *CCDC39* and *CCDC40* are the major cause of primary ciliary dyskinesia with axonemal disorganisation and absent inner dynein arms. *Hum Mutat* 2013;34:462–472.
34. Austin-Tse C, Halbritter J, Zariwala MA, Gilberti RM, Gee HY, Hellman N, Pathak N, Liu Y, Panizzi JR, Patel-King RS, *et al*. Zebrafish ciliopathy screen plus human mutational analysis identifies *C21orf59* and *CCDC65* defects as causing primary ciliary dyskinesia. *Am J Hum Genet* 2013;93:672–686.
35. Kott E, Legendre M, Copin B, Papon JF, Dastot-Le Moal F, Montantin G, Duquesnoy P, Piterboth W, Amram D, Bassinet L, *et al*. Loss-of-function mutations in *RSPH1* cause primary ciliary dyskinesia with central-complex and radial-spoke defects. *Am J Hum Genet* 2013; 93:561–570.
36. Leigh MW, Hazucha MJ, Chawla KK, Baker BR, Shapiro AJ, Brown DE, Lavange LM, Horton BJ, Qaqish B, Carson JL, *et al*. Standardizing nasal nitric oxide measurement as a test for primary ciliary dyskinesia. *Ann Am Thorac Soc* 2013;10:574–581.
37. Fu W, O'Connor TD, Jun G, Kang HM, Abecasis G, Leal SM, Gabriel S, Rieder MJ, Altshuler D, Shendure J, *et al*.; NHLBI Exome Sequencing Project. Analysis of 6,515 exomes reveals the recent origin of most human protein-coding variants. *Nature* 2013;493: 216–220.
38. Li H, Durbin R. Fast and accurate short read alignment with Burrows-Wheeler transform. *Bioinformatics* 2009;25:1754–1760.
39. McKenna A, Hanna M, Banks E, Sivachenko A, Cibulskis K, Kernytsky A, Garimella K, Altshuler D, Gabriel S, Daly M, *et al*. The Genome Analysis Toolkit: a MapReduce framework for analyzing next-generation DNA sequencing data. *Genome Res* 2010;20: 1297–1303.
40. Day A, Carlson MR, Dong J, O'Connor BD, Nelson SF. Celsius: a community resource for Affymetrix microarray data. *Genome Biol* 2007;8:R112.
41. Halbritter J, Diaz K, Chaki M, Porath JD, Tarrier B, Fu C, Innis JL, Allen SJ, Lyons RH, Stefanidis CJ, *et al*. High-throughput mutation analysis in patients with a nephronophthisis-associated ciliopathy applying multiplexed barcoded array-based PCR amplification and next-generation sequencing. *J Med Genet* 2012; 49:756–767.

42. Zhou H, Wang X, Brighton L, Hazucha M, Jaspers I, Carson JL. Increased nasal epithelial ciliary beat frequency associated with lifestyle tobacco smoke exposure. *Inhal Toxicol* 2009;21: 875–881.
43. Suprynowicz FA, Upadhyay G, Krawczyk E, Kramer SC, Hebert JD, Liu X, Yuan H, Cheluvaraju C, Clapp PW, Boucher RC Jr, *et al*. Conditionally reprogrammed cells represent a stem-like state of adult epithelial cells. *Proc Natl Acad Sci USA* 2012;109:20035–20040.
44. Fulcher ML, Gabriel S, Burns KA, Yankaskas JR, Randell SH. Well-differentiated human airway epithelial cell cultures. *Methods Mol Med* 2005;107:183–206.
45. Quanjer PH, Stanojevic S, Cole TJ, Baur X, Hall GL, Culver BH, Enright PL, Hankinson JL, Ip MS, Zheng J, *et al*.; ERS Global Lung Function Initiative. Multi-ethnic reference values for spirometry for the 3-95-yr age range: the global lung function 2012 equations. *Eur Respir J* 2012;40:1324–1343.
46. Papon JF, Coste A, Roudot-Thoraval F, Boucherat M, Roger G, Tamalet A, Vojtek AM, Amselem S, Escudier E. A 20-year experience of electron microscopy in the diagnosis of primary ciliary dyskinesia. *Eur Respir J* 2010;35:1057–1063.
47. Hirokawa N, Tanaka Y, Okada Y. Cilia, KIF3 molecular motor and nodal flow. *Curr Opin Cell Biol* 2012;24:31–39.
48. Yang P, Diener DR, Yang C, Kohno T, Pazour GJ, Dienes JM, Agrin NS, King SM, Sale WS, Kamiya R, *et al*. Radial spoke proteins of *Chlamydomonas* flagella. *J Cell Sci* 2006;119:1165–1174.
49. Shetty J, Klotz KL, Wolkowicz MJ, Flickinger CJ, Herr JC. Radial spoke protein 44 (human meichroacidin) is an axonemal alloantigen of sperm and cilia. *Gene* 2007;396:93–107.
50. Ostrowski LE, Blackburn K, Radde KM, Moyer MB, Schlatzer DM, Moseley A, Boucher RC. A proteomic analysis of human cilia: identification of novel components. *Mol Cell Proteomics* 2002;1: 451–465.